AGU PUBLICATIONS

Geophysical Research Letters

RESEARCH LETTER
10.1002/2015GL064075

Key Points:
- Solar radiation patterns have scale-dependent effects on streamflow generation
- The control is exerted by catchment size as opposed to aspect correlation scale
- The scale dependence affects the spatial transferability of degree-day factors

Supporting Information:
- Figures S1 and S2 and Text S1

Correspondence to:
F. Comola,
francesco.comola@epfl.ch

Citation:
Comola, F., B. Schaefli, P. Da Ronco, G. Botter, M. Bavay, A. Rinaldo, and M. Lehning (2015), Scale-dependent effects of solar radiation patterns on the snow-dominated hydrologic response, *Geophys. Res. Lett.*, *42*, 3895–3902, doi:10.1002/2015GL064075.

Received 31 MAR 2015
Accepted 4 MAY 2015
Accepted article online 11 MAY 2015
Published online 1 MAY 2015

Scale-dependent effects of solar radiation patterns on the snow-dominated hydrologic response

F. Comola[1], B. Schaefli[1], P. Da Ronco[2,3], G. Botter[4], M. Bavay[5], A. Rinaldo[1,4], and M. Lehning[1,5]

[1]School of Architecture, Civil and Environmental Engineering, École Polytechnique Fédérale de Lausanne, Lausanne, Switzerland, [2]Impacts on Soil and Coasts Division, Centro Euro-Mediterraneo sui Cambiamenti Climatici, Capua, Italy, [3]Department of Civil and Environmental Engineering, Politecnico di Milano, Milan, Italy, [4]Dipartimento di Ingegneria Civile, Edile ed Ambientale, Universitá degli Studi di Padova, Padua, Italy, [5]WSL Institute for Snow and Avalanche Research SLF, Davos, Switzerland

Abstract Solar radiation is a dominant driver of snowmelt dynamics and streamflow generation in alpine catchments. A better understanding of how solar radiation patterns affect the hydrologic response is needed to assess when calibrated temperature-index models are likely to be spatially transferable for ecohydrological applications. We induce different solar radiation patterns in a Swiss Alpine catchment through virtual rotations of the digital elevation model. Streamflow simulations are performed at different spatial scales through a spatially explicit hydrological model coupled to a physically based snow model. Results highlight that the effects of solar radiation patterns on the hydrologic response are scale dependent, i.e., significant at small scales with predominant aspects and weak at larger scales where aspects become uncorrelated and orientation differences average out. Such scale dependence proves relevant for the spatial transferability of a temperature-index model, whose calibrated degree-day factors are stable to different solar radiation patterns for catchment sizes larger than the aspect correlation scale.

1. Introduction

Understanding the hydrologic response of snow-dominated catchments is crucial for water resources management of many dry lowland regions where a large amount of water supply is provided during the snowmelt season [*Barnett et al.*, 2005]. Timing and magnitude of streamflow generation in alpine catchments is strongly related to the spatial and temporal variability of snow depth and ablation [*Grünewald et al.*, 2010], which interact in controlling the spatial pattern of snow water equivalent (SWE). The recent work of *Clark et al.* [2011] extensively reviewed the dominant processes controlling SWE distribution in alpine catchments, i.e., snow drifting [*Schirmer et al.*, 2011], preferential deposition [*Mott and Lehning*, 2010], vegetation [*Trujillo et al.*, 2009], melt energy [*DeBeer and Pomeroy*, 2010], and climate [*Trujillo and Molotch*, 2014]. *Pomeroy et al.* [2003] and *Ellis et al.* [2013] observed that the SWE distribution is significantly influenced by hillsope aspect, which acts as a main control on incoming solar radiation [see, e.g., *Garnier and Ohmura*, 1968].

The influence of catchment geomorphology has also been widely investigated in relation to rainfall-runoff transformation [e.g., *Rodríguez-Iturbe and Valdes*, 1979; *Gupta et al.*, 1980; *Rinaldo et al.*, 2006]. The structural complexity of the river network, i.e., the heterogeneity of paths available for hydrologic runoff, generates the so-called geomorphologic dispersion [*Rinaldo et al.*, 1991; *Rinaldo and Rodriguez-Iturbe*, 1996]. This effect sums up to the kinematic dispersion, which stems from the systematic variability of the advective transport processes, becoming asymptotically predominant when the basin scale becomes much larger than the mean hillslope size [*Saco and Kumar*, 2002; *Botter and Rinaldo*, 2003]. More recently, signatures of catchment geomorphology were investigated for base flow recession curves [*Biswal and Marani*, 2010; *Mutzner et al.*, 2013], for streamflow peaks [*Rigon et al.*, 2011], and for nonstationarity in flood frequency [*Slater et al.*, 2015].

The control exerted by a branching river network on the snowmelt-driven hydrologic response of alpine catchments has, however, not been studied so far. The presence of such a network may be particularly effective in connecting different source areas and in averaging out the heterogeneity of snowmelt processes. We therefore investigate whether the spatial distribution of solar radiation, altered artificially by virtual rotations of the digital elevation model (DEM), leaves a detectable hydrologic signature at different spatial scales. We conduct the study by applying a spatially explicit hydrologic response model coupled to a detailed physical

snow model. The relevance of this study is both theoretical, as the link between solar radiation distribution and hydrologic response is still largely unexplored, and practical, as it explains why carefully calibrated temperature-index models [*Hock*, 2003], in which the aspect is not explicitly accounted for, may be spatially transferable when applied to sufficiently large catchments.

In section 2, we introduce the modeling approach and the virtual experiments carried out to investigate the scale-dependent signature of radiation patterns. Section 3 describes the case study of the Alpine Dischma catchment (Grisons, Switzerland) and the model setup. Section 4 presents the results and discusses the role of solar radiation patterns in relation to different spatial scales.

2. Methods

2.1. Modeling Approach

Alpine3D is the fully distributed physically based model of snow processes developed at the WSL Institute for Snow and Avalanche Research, SLF (Davos, Switzerland). The meteorological data measured by automatic weather stations are spatially interpolated with the MeteoIO library [*Bavay and Egger*, 2014] to provide the necessary boundary conditions. The near surface processes are modeled based on a DEM and a land use model, whose resolution determines the size of the cells for the surface disctretization. Alpine3D consists of two three-dimensional modules, i.e., the radiation balance model and the snow drift model, and of the one-dimensional module Snowpack [*Schmucki et al.*, 2014], which simulates vertical transport of mass and energy in vegetation, snow, and soil for every cell of the grid. All these model components are described in detail in *Lehning et al.* [2006]. In particular, the radiation module is based on the so-called view-factor approach, which allows for a physically based simulation of the radiation balance on steep terrains in combination with spatially distributed information of surface processes [*Helbig et al.*, 2010]. The snow transport module, introduced by *Lehning et al.* [2008], simulates the saltation process with the equilibrium saltation model of *Doorschot et al.* [2004] and the advection-diffusion process with the streamline upwind Petrov-Galerkin technique [*Brooks and Hughes*, 1982]. The one-dimensional Snowpack model predicts snow development with fine stratigraphic details, solving the heat transport equation and the Richards equation in the vertical direction using a finite element method [*Wever et al.*, 2014]. Snowpack has been extended with a canopy module based on the big leaf concept, which simulates radiative and turbulent heat exchange between the vegetation and the snow/soil surface, evaporation of intercepted water, transpiration, and evaporation from the land surface [*Musselman et al.*, 2012; *Gouttevin et al.*, 2015]. The spatially explicit hydrologic module, described in detail in *Comola et al.* [2015] transforms the sequence of snowmelt pulses into streamflow time series at all nodes along the river network. The underlying hydrological processes are described by mass balance equations at subcatchment scale, i.e., within the catchment portions draining into individual reaches of the network. The model hinges on the stream network delineation provided by the analysis of the DEM and can thus account for arbitrary degrees of geomorphological complexity. The formulation of water transport is based on a travel time framework, accounting for water moisture dynamics and water age mixing processes [*Botter et al.*, 2010]. The mean travel times are assumed to scale with the subcatchment area according to *Alexander* [1972] and *Pilgrim et al.* [1982]. Although the full snow transport module is not used for hydrological applications due to the very high resolution and computing capacity required, Alpine3D has been shown to provide reliable snowmelt predictions in numerous studies related to snow hydrology [see, e.g., *Bavay et al.*, 2009, 2013].

2.2. Virtual Experiments

The effect of solar radiation patterns on the hydrologic response is analyzed through virtual experiments where the reference DEM of the catchment is rotated maintaining the relative positions of the weather stations. Accordingly, every rotation changes the aspects of the hillslope pixels and thus the pattern of incoming solar radiation, but preserves the spatial distribution of the other meteorological variables, i.e., wind speed and direction, air temperature, soil temperature, longwave radiation, relative humidity, and precipitation. This procedure results in different spatial distributions of snowmelt but does not affect the snow accumulation pattern. We rotate the DEM of the study catchment 3 times by 90° and simulate snowmelt dynamics and streamflow generation in the four resulting configurations. A similar rotation procedure was also adopted by *Taesam et al.* [2015] to study the directional influence of moving storms on basin response. It is noteworthy that, in real environments, different slope configurations also affect wind and deposition patterns, inducing aspect-dependent differences in vegetation and soil development, with relevant hydrologic implications.

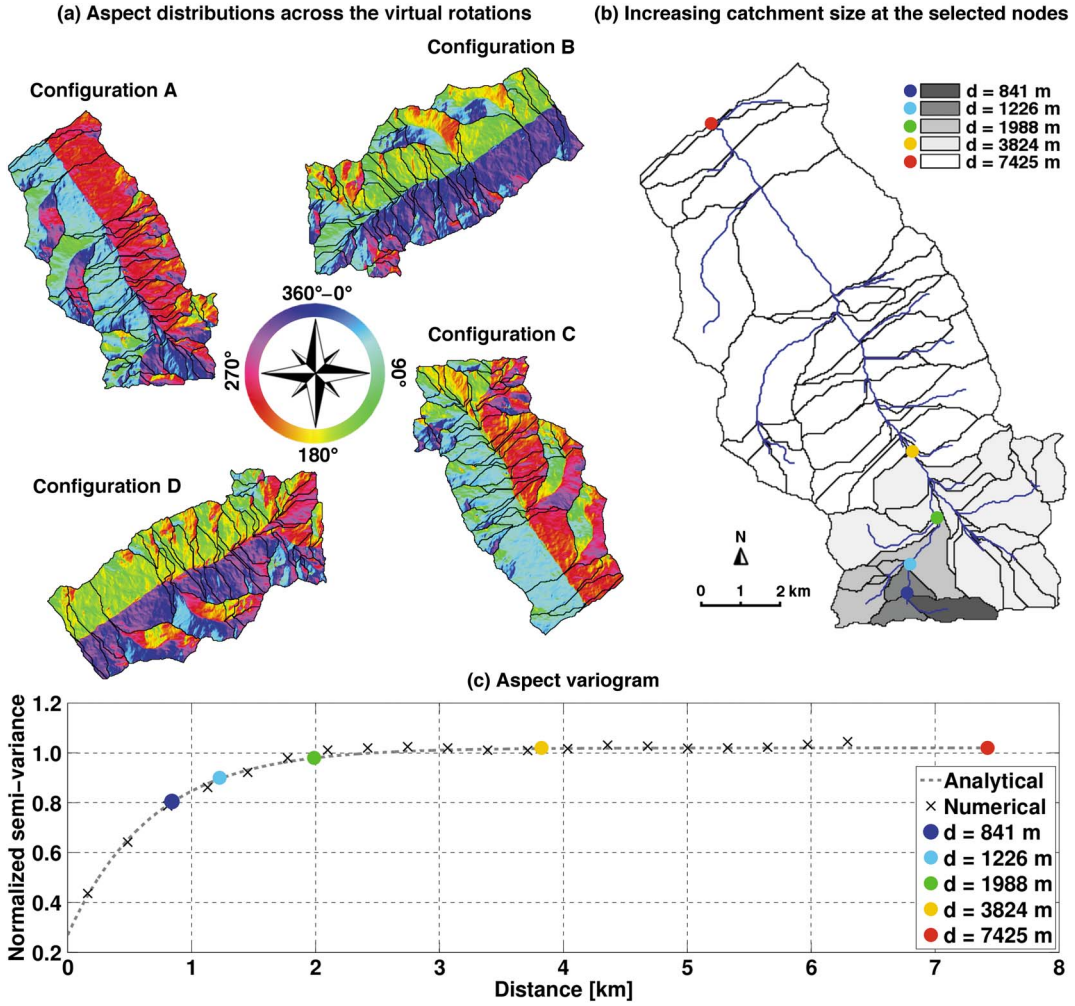

Figure 1. (a) Digital maps of aspects in the original orientation of the catchment and after applying rotations of 90°, 180°, and 270°. In the text, we refer to these orientations as configurations A, B, C, and D. (b) Series of nested catchment portions, for which the effect of solar radiation patterns is analyzed, and corresponding characteristic size d (see text for details on its computation). (c) Numerical and analytical variograms of aspect spatial field, normalized with respect to the total variance of the aspect field.

The scale-dependent effect on the hydrologic response is analyzed by simulating the streamflow at selected network nodes that drain progressively larger areas of the catchment. Each of these nodes drains a well-defined catchment having a characteristic size d (m) related to its drainage area A (m^2) according to the relation $d = \sqrt{4A/\pi}$. Accordingly, d is the diameter of the equivalent circular shape of the drained area. Regardless of the proportionality constant, $d \propto \sqrt{A}$ is a scaling expression commonly used to compare the characteristic size of a catchment to the spatial scale of the meteorological forcing. *Nicótina et al.* [2008] adopted, for instance, a similar approach to study the influence of rainfall spatial correlation on the hydrologic response. Here we compare the characteristic size d to the correlation scale of the pixel aspects, which represents the distance at which the maximum spatial variability of aspects is sampled. A commonly used tool to estimate the correlation scale of random fields is the variogram [*Tate and Atkinson*, 2001], which can be numerically computed based on DEMs.

3. Case Study and Simulation Setup

The Dischma catchment spans 43.3 km^2 and is located in the Swiss Alps. The outlet is located at Dischma Kriegsmatte and the elevation ranges from 1677 to 3130 m. Thirty-six percent of the land surface is covered by alpine meadows, 34% is rock covered, and the remaining fraction is mainly occupied by forest and bushes; 2%

of the catchment area is currently glacier covered (more detailed information on the catchment can be found in, e.g., *Zappa et al.* [2003]). The absence of large forested areas in the catchment reduces the sources of variability of incoming radiation [see, e.g., *Musselman et al.*, 2013] and establishes a more direct connection between aspect and radiation patterns. In the first Alpine3D study, *Lehning et al.* [2006] already showed the substantial influence of the topography-controlled solar radiation pattern on the snowmelt in the Dischma catchment.

The aspect maps for the four studied solar radiation distributions, which will be addressed hereafter as configurations A, B, C, and D, are given in Figure 1a. The geomorphological analysis of the catchment is performed with the Taudem routines [*Tarboton*, 1997], applied to a 25 m resolution DEM, and delineates a stream network with 55 subcatchments (Figure 1b).

An Alpine3D simulation is carried out for the period October 2004 to October 2005, such that a snow-free surface can be prescribed as initial condition. The small glaciated area is initialized by providing ice depth at the corresponding pixels. The study catchment is discretized with squared elements of 100 m side length. The spatial distribution of the meteorological forcings, performed with a Kriging geostatistics interpolation, hinges on the hourly records of 18 high Alpine automatic weather and snow stations (Interkantonales Mess- und Informationssystem, IMIS), deployed in the area by the WSL Institute for Snow and Avalanche Research (SLF) in cooperation with the Swiss mountain cantons. The hydrologic response module runs with the parameter set reported in *Comola et al.* [2015], which was calibrated for the year 2012 against the streamflow at the outlet of the Dischma catchment and validated for the year 2013.

The progressively larger catchment portions considered in the analysis of the scale dependance are shown in Figure 1b, together with the corresponding size d. Catchment portions having darker colors are nested within the ones having lighter color, such that the drainage area progressively increases along the selected nodes. Even though streamflow measurements were not available for all the selected sections, the model setup can confidently provide reliable streamflow simulations at the intermediate network nodes owing to the physical description of distributed snow processes and the spatially explicit setup that accounts for drainage areas in the scaling of the travel times.

4. Results and Discussion

Figure 1c shows the numerical variogram along with a fitted exponential model for visualization purposes. In the computation of the numerical variogram, the aspect field is treated as isotropic [*Cressie and Cassie*, 1993]. This procedure provides a simple yet meaningful estimation of the correlation scale. Figure 1c shows that the variance reaches a threshold at distances of the order of 3 km ($A \simeq 7$ km^2). The nodes corresponding to the first three catchment portions analyzed lie below this threshold, while the characteristic size of the fourth one is approximately equal to this correlation scale. The variograms computed for other catchments of similar size in the Swiss Alps present similar trends (see supporting information), suggesting that the decorrelation of aspects at certain scales is a typical feature in Alpine environments. The numerical variogram shown in Figure 1c is obtained by applying a random sampling to all pixels. This sampling technique is known to be the source of spurious nugget effects, as visible in Figure 1c at short lags, which however does not affect the estimation of the correlation scale [*Weng*, 2002].

The results in terms of specific streamflow are shown in Figure 2, where the signals during the snowmelt phase are given for the different catchment configurations and spatial scales. We observe that, at the smallest scale (Figure 2a), the effect of solar radiation distribution is evident during both the two major streamflow events, having their peaks in late May and late June, respectively. As shown in Figure 1a, the considered subcatchment is forced to change from east facing, to north, west, and south facing through the three rotations. In May, when snowmelt is only energy limited, the streamflow increases as a function of the incoming solar radiation. Accordingly, the largest streamflow increase is observed for the east and south facing configurations (A and D), showing values up to 50% larger than the north facing and west facing configurations (B and C) at the end of May. In June, instead, snowmelt is partly energy limited and partly limited by the available snow. The largest streamflow occurs, in fact, for the north and west facing configurations (B and C), which receive less energy but have more snow available due to lower melt during the previous event. During this second streamflow event, the maximum difference among the tested configurations occurs at the end of June and is estimated around 30%.

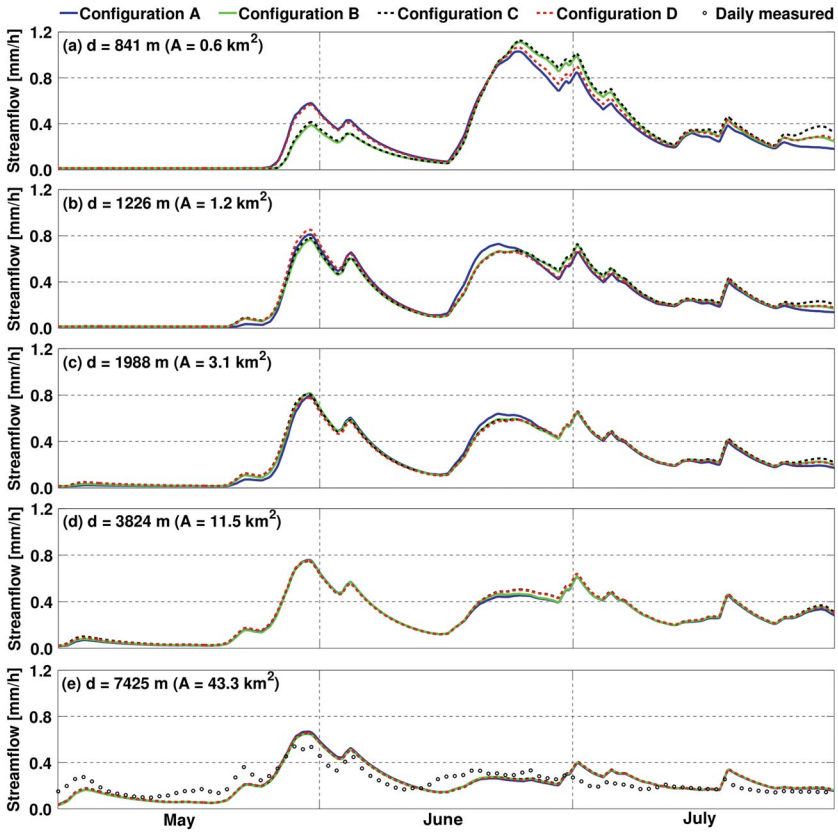

Figure 2. (a–e) Hydrologic response in the four different configurations and for progressively larger catchment portions. The results are given in terms of specific streamflow per unit catchment area during the melting season of the year 2005. Signals are averaged over 24 h.

The above analysis illustrates how the interplay of energy limitation and storage limitation influences the hydrologic response of a subcatchment with a dominant aspect. At progressively increasing spatial scales, the distribution of the aspect is more heterogeneous, thereby preventing a straightforward interpretation of the results. Nevertheless, Figure 2b shows that the hydrologic response is still sensitive to the spatial distribution of solar radiation up to a scale of around 1.2 km ($A \simeq 1$ km^2), where the combined effects of energy and storage limitation enhances the differences among the configurations. Figure 2c shows that at scales of around 2.0 km ($A \simeq 3$ km^2) the differences in the two snowmelt peaks become very small. At scales of around 3.8 km ($A \simeq 11$ km^2), small variations are visible only during the second snowmelt peak (Figure 2d) and they completely disappear at larger scales (Figure 2e). Here the size of the catchment is such that the spatial variability of aspects is fully sampled in all the tested configurations.

Accordingly, we argue that different spatial patterns of snowmelt resulting from different distributions of solar radiation do not influence catchment-scale streamflows, provided that the drainage area is large enough with respect to the aspect correlation scale. These observations are similar to the results obtained by *Nicótina et al.* [2008], who analyzed the impact of different rainfall patterns on the hydrologic response at catchment scale. They observed that, for catchments where Hortonian overland flow is negligible, the exact spatial distribution of rainfall is immaterial to the streamflow signal at the outlet, provided that the rainfall spatial average is conserved.

To provide a deeper insight into the observed scale dependence, we averaged in time the spatially distributed values of incoming solar radiation, snowmelt, and specific streamflow during the peak of the first snowmelt event (25 May to 1 June) and plotted the corresponding coefficient of variation across the four different configurations (Figure 3). The coefficient of variation of SWE is shown and discussed in the supporting information. Significant variations in the solar radiation pattern occur across the ridges of the catchment (Figure 3a), where the terrain is steeper and aspects change significantly as a result of the rotations, while almost no differences are observed at the bottom of the valley. Accordingly, a similar pattern is observed for the coefficient of varia-

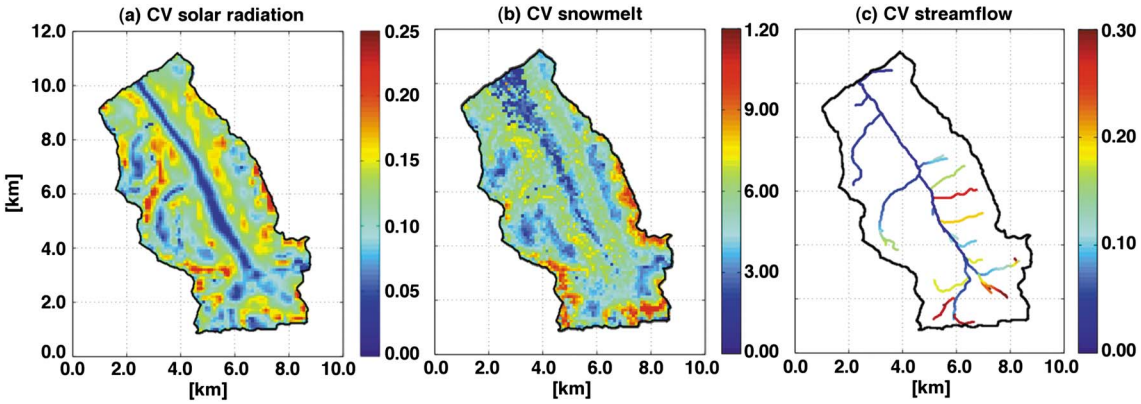

Figure 3. Coefficient of variation, across the four tested configurations, of (a) the incoming solar radiation field, (b) the snowmelt field, and (c) the specific streamflow along the network. The values refer to the time averaged values of the first snowmelt peak 25 May to 1 June.

tion of snowmelt (Figure 3b). Figure 3c suggests that headwater streams generally exhibit a larger coefficient of variation, and therefore a large sensitivity to changes in solar radiation patterns, which is thereafter progressively lost toward the outlet. Figure 4a shows the coefficient of variation of specific streamflow at the nodes of the river network versus the catchment size at the corresponding nodes. It is observed that different solar radiation patterns have an influence on the hydrologic response up to a characteristic catchment size of the order of the aspect correlation scale. The reason of the scatter observed for small catchment sizes lies in the slope-dependent aspect variations induced by the DEM rotations. Accordingly, these rotations produce larger streamflow variations in steep subcatchments.

The relevant implications on the spatial transferability of temperature-index models are shown by applying the spatially explicit model SEHR-ECHO, described in detail in *Schaefli et al.* [2014], which simulates the snow processes through a simple degree-day approach. In a first stage, all the 12 parameters of SEHR-ECHO were calibrated to match the streamflow computed by Alpine3D at the catchment outlet during the year 2005. For this calibration, the parameter set that maximizes the Nash-Sutcliffe efficiency is chosen among 35,000 randomly generated parameter sets. In a second step, a degree-day factor is calibrated for each network node by maximizing the Nash-Sutcliffe efficiency computed on the log-transformed streamflows, in order to reduce the spurious sensitivity to rainfall-driven peak flows. We repeated this second step for all the four configurations, A, B, C, and D, and plotted the corresponding degree-day factors as a function of the catchment size in Figure 4b. Results highlight that the calibrated degree-day factors are sensitive to solar radiation

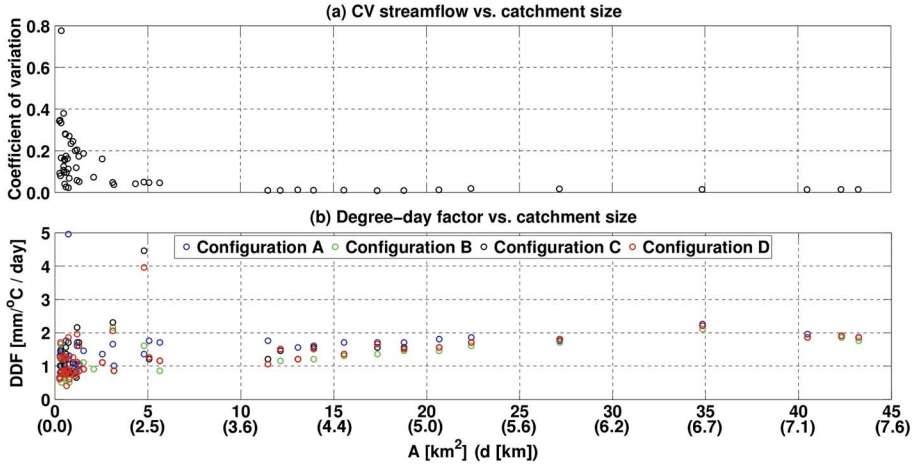

Figure 4. (a) Coefficient of variation of specific streamflow, as provided by Alpine3D at all nodes of the network, and (b) degree-day factors of the spatially explicit hydrological model SEHR-ECHO [see *Schaefli et al.*, 2014], calibrated to match the streamflow computed by Alpine3D, versus the catchment size at the corresponding nodes. The catchment size is given both in terms of drainage area *A* and characteristic size *d* for comparison with the aspect correlation scale. Only the points corresponding to a Nash-Sutcliffe efficiency higher than 0.5 are shown (94% of the total).

distribution at small scales, where points belonging to different configurations are spread out, while they stabilize at catchment sizes of the order of the aspect correlation scale. Previous studies have investigated the sources of variability in the degree-day factors, identifying solar radiation as one of the most relevant [see, e.g., *He et al.*, 2014, and references herein]. Therefore, we argue that the stabilization of the degree-day factors beyond the aspect correlation scale is strictly related to the scale-dependent effects of solar radiation patterns on the hydrologic response.

5. Conclusions

This paper investigated the role of solar radiation distribution in the hydrologic response of Alpine catchments characterized by progressively larger drainage areas. The study was carried out numerically with a spatially explicit hydrological model coupled to a physically based snow model. Different solar radiation distributions were induced by virtual rotation of the catchment DEM. The relative positions of the meteorological stations were preserved in the rotations in order to change the snowmelt pattern without influencing the snow accumulation distribution.

The spatial analysis of the simulated streamflows showed that the signature of solar radiation patterns on the hydrologic response is scale dependent, i.e., significant when the characteristic size of the catchment is smaller than the correlation scale of the aspects and almost inexistent when the catchment size is larger. Our analysis also suggested that such scale dependence has an impact on the calibration of temperature-index models, whose degree-day factors might show variability at small scales but stabilize for catchment sizes larger than the correlation scale of aspects. Even though the presence of large forested areas may introduce an additional source of variability for the distribution of incoming solar radiation, and therefore for the degree-day factors, the results suggest that different solar radiation patterns do not impair the spatial transferability of temperature-index models for hydrological simulations of catchments larger than a reference length scale defined by their aspect spatial distribution.

Acknowledgments

The authors thank the two anonymous reviewers for their constructive comments. The streamflow data were obtained from the Swiss Federal Office for the Environment. The meteorological data was obtained from the IMIS (Interkantonales Mess- und Informationssystem) network, MeteoSwiss, and SLF stations. Data used in this study can be made available upon request.

The Editor thanks two anonymous reviewers for their assistance in evaluating this paper.

References

Alexander, G. (1972), Effect of catchment area on flood magnitude, *J. Hydrol.*, *16*(3), 225–240, doi:10.1016/0022-1694(72)90054-6.

Barnett, T., J. Adam, and D. Lettenmaier (2005), Potential impacts of a warming climate on water availability in snow-dominated regions, *Nature*, *438*(7066), 303–309, doi:10.1038/nature04141.

Bavay, M., M. Lehning, T. Jonas, and H. Löwe (2009), Simulations of future snow cover and discharge in Alpine headwater catchments, *Hydrol. Proc.*, *23*(1), 95–108, doi:10.1002/hyp.7195.

Bavay, M., T. Grünewald, and M. Lehning (2013), Response of snow cover and runoff to climate change in high Alpine catchments of eastern Switzerland, *Adv. Water Resour.*, *55*(0), 4–16, doi:10.1016/j.advwatres.2012.12.009.

Bavay, M., and T. Egger (2014), MeteoIO 2.4.2: A preprocessing library for meteorological data, *Geosci. Model Dev.*, *7*, 3135–3151, doi:10.5194/gmd-7-3135-2014.

Biswal, B., and M. Marani (2010), Geomorphological origin of recession curves, *Geophys. Res. Lett.*, *37*, L24403, doi:10.1029/2010GL045415.

Botter, G., and A. Rinaldo (2003), Scale effect on geomorphologic and kinematic dispersion, *Water Resour. Res.*, *39*(10), 1286, doi:10.1029/2003WR002154.

Botter, G., E. Bertuzzo, and A. Rinaldo (2010), Transport in the hydrologic response: Travel time distributions, soil moisture dynamics, and the old water paradox, *Water Resour. Res.*, *46*, W03514, doi:10.1029/2009WR008371.

Brooks, A. N., and T. J. R. Hughes (1982), Streamline upwind/Petrov-Galerkin formulations for convection dominated flows with particular emphasis on the incompressible Navier-Stokes equations, *Comput. Method. Appl. Mech.*, *32*(1), 199–259, doi:10.1016/0045-7825(82)90071-8.

Clark, M. P., J. Hendrikx, A. G. Slater, D. Kavetski, B. Anderson, N. J. Cullen, T. Kerr, E. Örn Hreinsson, and R. A. Woods (2011), Representing spatial variability of snow water equivalent in hydrologic and land-surface models: A review, *Water Resour. Res.*, *47*, W07539, doi:10.1029/2011WR010745.

Comola, F., B. Schaefli, A. Rinaldo, and M. Lehning (2015), Thermodynamics in the hydrologic response: Travel time formulation and application to Alpine catchments, *Water Resour. Res.*, *51*, 1671–1687, doi:10.1002/2014WR016228.

Cressie, N. A., and N. A. Cassie (1993), *Statistics for Spatial Data*, vol. 900, Wiley, New York.

DeBeer, C. M., and J. W. Pomeroy (2010), Simulation of the snowmelt runoff contributing area in a small alpine basin, *Hydrol. Earth Syst. Sc.*, *14*(7), 1205–1219, doi:10.5194/hess-14-1205-2010.

Doorschot, J. J., M. Lehning, and A. Vrouwe (2004), Field measurements of snow-drift threshold and mass fluxes, and related model simulations, *Boundary Layer Meteorol.*, *113*(3), 347–368, doi:10.1007/s10546-004-8659-z.

Ellis, C. R., J. W. Pomeroy, and T. E. Link (2013), Modeling increases in snowmelt yield and desynchronization resulting from forest gap-thinning treatments in a northern mountain headwater basin, *Water Resour. Res.*, *49*(2), 936–949, doi:10.1002/wrcr.20089.

Garnier, B. J., and A. Ohmura (1968), A method of calculating the direct shortwave radiation income of slopes, *J. Appl. Meteorol.*, *7*(5), 796–800, doi:10.1175/1520-0450(1968)007<0796:AMOCTD>2.0.CO;2.

Gouttevin, I., M. Lehning, T. Jonas, D. Gustafsson, and M. Mölder (2015), A two-layer canopy with thermal inertia for an improved modelling of the sub-canopy snowpack energy-balance, *Geosci. Model Dev. Discuss.*, *8*(1), 209–262, doi:10.5194/gmdd-8-209-2015.

Grünewald, T., M. Schirmer, R. Mott, and M. Lehning (2010), Spatial and temporal variability of snow depth and ablation rates in a small mountain catchment, *Cryosphere*, *4*(2), 215–225, doi:10.5194/tc-4-215-2010.

Gupta, V. K., E. Waymire, and C. Wang (1980), A representation of an instantaneous unit hydrograph from geomorphology, *Water Resour. Res.*, *16*(5), 855–862.

He, Z. H., J. Parajka, F. Q. Tian, and G. Blöschl (2014), Estimating degree-day factors from MODIS for snowmelt runoff modeling, *Hydrol. Earth Syst. Sc.*, *18*(12), 4773–4789, doi:10.5194/hess-18-4773-2014.
Helbig, N., H. Loewe, B. Mayer, and M. Lehning (2010), Explicit validation of a surface shortwave radiation balance model over snow-covered complex terrain, *J. Geophys. Res.*, *115*, D18113, doi:10.1029/2010JD013970.
Hock, R. (2003), Temperature index melt modelling in mountain areas, *J. Hydrol.*, *282*(1), 104–115, doi:10.1016/S0022-1694(03)00257-9.
Lehning, M., I. Völksch, D. Gustafsson, T. Nguyen, M. Stähli, and M. Zappa (2006), ALPINE3D: A detailed model of mountain surface processes and its application to snow hydrology, *Hydrol. Proc.*, *20*(10), 2111–2128, doi:10.1002/hyp.6204.
Lehning, M., H. Löwe, M. Ryser, and N. Raderschall (2008), Inhomogeneous precipitation distribution and snow transport in steep terrain, *Water Resour. Res.*, *44*, W07404, doi:10.1029/2007WR006545.
Mott, R., and M. Lehning (2010), Meteorological modeling of very high-resolution wind fields and snow deposition for mountains, *J. Hydrometeorol.*, *11*(4), 934–949.
Musselman, K. N., N. P. Molotch, S. A. Margulis, M. Lehning, and D. Gustafsson (2012), Improved snowmelt simulations with a canopy model forced with photo-derived direct beam canopy transmissivity, *Water Resour. Res.*, *48*, W10509, doi:10.1029/2012WR012285.
Musselman, K. N., S. A. Margulis, and N. P. Molotch (2013), Estimation of solar direct beam transmittance of conifer canopies from airborne LiDAR, *Remote Sens. Environ.*, *136*(0), 402–415, doi:10.1016/j.rse.2013.05.021.
Mutzner, R., E. Bertuzzo, P. Tarolli, S. Weijs, L. Nicotina, S. Ceola, N. Tomasic, I. Rodriguez-Iturbe, M. Parlange, and A. Rinaldo (2013), Geomorphic signatures on Brutsaert base flow recession analysis, *Water Resour. Res.*, *49*(9), 5462–5472, doi:10.1002/wrcr.20417.
Nicótina, L., E. Alessi Celegon, A. Rinaldo, and M. Marani (2008), On the impact of rainfall patterns on the hydrologic response, *Water Resour. Res.*, *44*, W12401, doi:10.1029/2007WR006654.
Pilgrim, D., I. Cordery, and B. Baron (1982), Effects of catchment size on runoff relationships, *J. Hydrol.*, *58*(3), 205–221, doi:10.1016/0022-1694(82)90035-X.
Pomeroy, J. W., B. Toth, R. J. Granger, N. R. Hedstrom, and R. L. H. Essery (2003), Variation in surface energetics during snowmelt in a subarctic mountain catchment, *J. Hydrometeorol.*, *4*(4), 702–719, doi:10.1175/1525-7541(2003)004<0702:VISEDS>2.0.CO;2.
Rigon, R., P. D'Odorico, and G. Bertoldi (2011), The geomorphic structure of the runoff peak, *Hydrol. Earth Syst. Sci.*, *15*(6), 1853–1863, doi:10.5194/hess-15-1853-2011.
Rinaldo, A., and I. Rodriguez-Iturbe (1996), Geomorphological theory of the hydrological response, *Hydrol. Proc.*, *10*(6), 803–829, doi:10.1002/(SICI)1099-1085(199606)10:6<803::AID-HYP373>3.0.CO;2-N.
Rinaldo, A., A. Marani, and R. Rigon (1991), Geomorphological dispersion, *Water Resour. Res.*, *27*(4), 513–525, doi:10.1029/90WR02501.
Rinaldo, A., G. Botter, E. Bertuzzo, A. Uccelli, T. Settin, and M. Marani (2006), Transport at basin scales: 1. Theoretical framework, *Hydrol. Earth Syst. Sc.*, *10*(1), 19–29, doi:10.5194/hess-10-19-2006.
Rodríguez-Iturbe, I., and J. B. Valdes (1979), The geomorphologic structure of hydrologic response, *Water Resour. Res.*, *15*(6), 1409–1420.
Saco, P. M., and P. Kumar (2002), Kinematic dispersion in stream networks 1. Coupling hydraulic and network geometry, *Water Resour. Res.*, *38*(11), 1244, doi:10.1029/2001WR000695.
Schaefli, B., L. Nicótina, C. Imfeld, P. Da Ronco, E. Bertuzzo, and A. Rinaldo (2014), SEHR-ECHO v1.0: A Spatially Explicit Hydrologic Response model for ecohydrologic applications, *Geosci. Model Dev.*, *7*(6), 2733–2746, doi:10.5194/gmd-7-2733-2014.
Schirmer, M., V. Wirz, A. Clifton, and M. Lehning (2011), Persistence in intra-annual snow depth distribution: 1. Measurements and topographic control, *Water Resour. Res.*, *47*, W09516, doi:10.1029/2010WR009426.
Schmucki, E., C. Marty, C. Fierz, and M. Lehning (2014), Evaluation of modelled snow depth and snow water equivalent at three contrasting sites in Switzerland using snowpack simulations driven by different meteorological data input, *Cold. Reg. Sci. Technol.*, *99*, 27–37, doi:10.1016/j.coldregions.2013.12.004.
Slater, L. J., M. B. Singer, and J. W. Kirchner (2015), Hydrologic versus geomorphic drivers of trends in flood hazard, *Geophys. Res. Lett.*, *42*, 370–376, doi:10.1002/2014GL062482.
Taesam, L., S. Juyoung, P. Taewoong, and L. Dongryul (2015), Basin rotation method for analyzing the directional influence of moving storms on basin response, *Stoch. Environ. Res. Risk Assess.*, 251–263, doi:10.1007/s00477-014-0870-y.
Tarboton, D. (1997), A new method for the determination of flow directions and upslope areas in grid digital elevation models, *Water Resour. Res.*, *33*(2), 309–319, doi:10.1029/96WR03137.
Tate, N. J., and P. M. Atkinson (2001), *Modelling Scale in Geographical Information Science*, John Wiley, Chichester, U. K.
Trujillo, E., and N. P. Molotch (2014), Snowpack regimes of the Western United States, *Water Resour. Res.*, *50*(7), 5611–5623, doi:10.1002/2013WR014753.
Trujillo, E., J. A. Ramírez, and K. J. Elder (2009), Scaling properties and spatial organization of snow depth fields in sub-alpine forest and alpine tundra, *Hydrol. Proc.*, *23*(11), 1575–1590, doi:10.1002/hyp.7270.
Weng, Q. (2002), Quantifying uncertainty of digital elevation models derived from topographic maps, in *Advances in Spatial Data Handling*, pp. 403–418, Springer, Berlin, doi:10.1007/978-3-642-56094-1_-30.
Wever, N., C. Fierz, C. Mitterer, H. Hirashima, and M. Lehning (2014), Solving Richards equation for snow improves snowpack meltwater runoff estimations in detailed multi-layer snowpack model, *Cryosphere*, *8*(1), 257–274, doi:10.5194/tc-8-257-2014.
Zappa, M., M. Pos, U. Strasser, P. Warmerdam, and J. Gurtz (2003), Seasonal water balance of an Alpine catchment as evaluated by different methods for spatially distributed snowmelt modelling, *Nord. Hydrol.*, *34*(3), 179–202.